Extended Abstracts of the 2018 International Conference on Solid State Devices and Materials, Tokyo, 2018, pp47-48

Properties of Shallow Nitrogen Vacancy Centers in Nitrogen Terminated Diamond and Detection of Nuclear Magnetic Resonance

Takahiro Sonoda[1], Sora Kawai[1], Hayate Yamano[1], Kanami Kato[1], Jorge J. Buendia[1], Taisuke Kageura[1], Yu Ishii[1], Kiro Nagaoka[1], Ryosuke Fukuda[1], Takuma Okada[1], Moriyoshi Haruyama[2, 3], Takashi Tanii[1], Keisuke Yamada[2], Shinobu Onoda[2], Wataru Kada[3], Osamu Hanaizumi[3], Alastair Stacey[4], Tokuyuki Teraji[5], Shozo Kono[7], Junichi Isoya[6], Hiroshi Kawarada[1, 7]

[1] Waseda University, 3-4-1, Okubo, Shinjuku-ku, Tokyo 169-8555, Japan
Phone: +81-3-5286-3391 E-mail: t-sonoda@suou.waseda.jp
[2] National Institute of Quantum and Radiological Science and Technology, [3] Gunma University,
[4] Melbourne University, [5] National Institute of Materials Science, [6] University of Tsukuba,
[7] Kagami Memorial Research Institute for Materials Science and Technology

Abstract

We investigated the characteristics of shallow NV centers under the nitrogen terminated surface of diamond. The N terminated surface was achieved by nitrogen radical beam exposure. We found that the negatively charged state was stabilized and the coherence time T_2 was comparable to that of the NV centers under the oxygen terminated surface. Furthermore, we successfully detected nuclear spin of ^{1}H by conducting XY8 measurement under the N terminated surface.

1. Introduction

Nitrogen vacancy (NV) centers in diamond have remarkable characteristics such as manipulation and readout of spin state and long spin coherence time T_2 (~ 2 ms [1]) in room temperature. One of the promising applications of NV centers is the nanoscale sensor for magnetic fields such as very weak magnetic field induced by nuclear spins [2]. Since signal strength decays as $1/r^3$, where r is the distance from the source of the magnetic field, near-surface NV centers need to be fabricated for the sensor applications. However, shallow NV centers have some limitations. One of the limitations is short spin coherence time T_2 compared to the NV centers in bulk diamond. Another limitation is that the negatively charged state of NV centers (NV^-) is unstable. To overcome these disadvantages, the surface terminations to change surface electric structure of diamond are attracting large interests. Two of the most common terminations are hydrogen termination and oxygen termination. NV^- is unstable under the H terminated surface, which exhibits a negative electron affinity [3]. On the other hand, NV^- is stable under the O terminated surface, which exhibits a positive electron affinity [4, 5]. As another termination, nitrogen-terminated surface is proposed. In the latest theoretical calculation, the N terminated surface was expected to show a positive electron affinity and contribute to NV^- stabilization and other positive effect to the property of the shallow NV centers [6]. Recently, we have actually achieved the N terminated surface by nitrogen radical beam exposure and confirmed that NV^- is stabilized under the N terminated surface [7]. Here, we further investigated about the effect of nitrogen termination on the shallow NV centers. Also, we found that the N terminated surface is advantageous for detection of nuclear spins such as ^{1}H placed on the surface.

2. Experimental Details

^{12}C enriched high purity diamond films were homoepitaxially grown on (001) diamond substrates [8]. Single NV centers were created by low energy ^{15}N ion implantation at 2.5 keV (average depth calculated by SRIM simulation [9]: 4.6 nm) and subsequent thermal annealing at 1000 ℃ for 2 hours [1]. The ^{15}N ion implantation was conducted through nano-hole resist masks made by electron beam lithography in order to create array of NV centers. Then, hot acid treatment was conducted for cleaning of the surface and oxygen termination. Formation of the N terminated surface was achieved by nitrogen radical beam exposure, which is generally used for molecular beam epitaxial (MBE) growth of III-nitride. The N radical beam does not produce surface damage. For N radical generation, two types of gases were flowed into RF plasma generator respectively to two samples: mixture gas of N_2 (96%) + H_2 (4%) for Sample N_2/H_2 and pure N_2 gas for Sample N_2.

A custom-built laser scanning confocal fluorescence microscope (CFM) was used for observation and evaluation of shallow single NV centers. Charge stability of NV^- was evaluated by the contrast of Rabi oscillation and spin coherence time T_2 was estimated by Hahn echo measurement. XY8 measurements were conducted to detect nuclear magnetic resonance (NMR) signals from ^{1}H nuclear spins in immersion oil using the single NV centers under the N terminated surface of Sample N_2/H_2.

3. Results and Discussions

Figure 1 shows distributions of the contrast of Rabi oscillation C after the N radical beam exposure on both samples. Here, C is defined as

$$C = \frac{F_{\mathrm{top}} - F_{\mathrm{bottom}}}{F_{\mathrm{middle}}} = \frac{2(F_{\mathrm{top}} - F_{\mathrm{bottom}})}{F_{\mathrm{top}} + F_{\mathrm{bottom}}}, \quad (1)$$

where F_{top}, F_{bottom}, and $F_{\mathrm{middle}} = (F_{\mathrm{top}} + F_{\mathrm{bottom}})/2$ are the normalized fluorescence intensities of the top, bottom, and middle of the Rabi oscillations. In the case of Sample N_2/H_2, average contrast C was 0.20 after the hot acid treatment and

0.38 after the N radical beam exposure (N_2 (96%) + H_2 (4%)). In the case of Sample N_2, average contrast C was 0.18 after the hot acid treatment and 0.33 after the N radical beam exposure (pure N_2). These results indicate that the N terminated surface contributes to NV^- stabilization. Figure 2 shows the result of estimation of coherence time T_2 after the N radical beam exposure on both samples. The longest coherence time was $T_2 \sim 30$ μs for Sample N_2/H_2 and $T_2 \sim 16$ μs for Sample N_2. A large portion of the estimated values were $T_2 \lesssim 5$ μs, which were comparable to those after the hot acid treatment for both samples.

Figure 3 shows the NMR spectra of ^{1}H nuclear spins detected by XY8-8 (64 π pulses) measurement using a single NV center under the N terminated surface of Sample N_2/H_2. Each spectrum in three different colors exhibits the result of XY8-8 measurements in three different magnitudes of applied static magnetic field. The vertical axis represents normalized contrast of NV fluorescence and the horizontal axis represents frequency of ^{1}H Larmor precession. The shifts of signal frequency corresponding to the variation of applied magnetic field indicate that the signals were derived from ^{1}H spins. Figure 4 shows coherence time T_2 estimated by Hahn echo measurement against depth of NV centers extracted from the NMR spectrum [10]. The positive correlation between T_2 and NV depth can be confirmed from these data. This will be the first report about the detection of NMR signal on nitrogen terminated surface.

4. Conclusions

Charge stability of shallow NV centers were improved by N radical beam exposure. Spin properties of shallow NV centers under N terminated surface were comparable to those under O terminated surface. NMR signal of ^{1}H was successfully detected on the N terminated surface.

Acknowledgements

This work was supported by JSPS Grant-in-Aid for Scientific Research (S) Grant Number 26220903 and Grant-in-Aid for Scientific Research (B) Grant number 15H03980. We thank Dr. Liam P. McGuinness and Professor Fedor Jelezko for their help with setting up the CFM.

References

[1] T. Yamamoto, J. Isoya, et al., Phys. Rev. B **88** (2013) 075206.
[2] T. Staudacher, J. Wrachtrup, et al., Science **339** (2013) 561.
[3] M. Hauf, J. Garrido, et al., Phys. Rev. B **83** (2011) 081304(R).
[4] F. F. de Oliveira, J. Wrachtrup, et al., Appl. Phys. Lett. **107** (2015) 073107.
[5] H. Yamano, H. Kawarada, et al., Jpn. J. Appl. Phys. **56** (2017) 04CK08.
[6] A. Stacey, S. Prawer, et al., Adv. Mater. Interfaces **2** (2015) 1500079.
[7] T. Kageura, H. Kawarada, et al, Appl. Phys. Express **10** (2017) 055503.
[8] T. Teraji, J. Appl. Phys. **118** (2015) 115304.
[9] J. F. Ziegler, et al., SRIM The Stopping and Range of Ions in Matter (SRIM Co., 2008).
[10] L. Pham, R. Walsworth, et al., Phys. Rev. B **93** (2016) 045425.

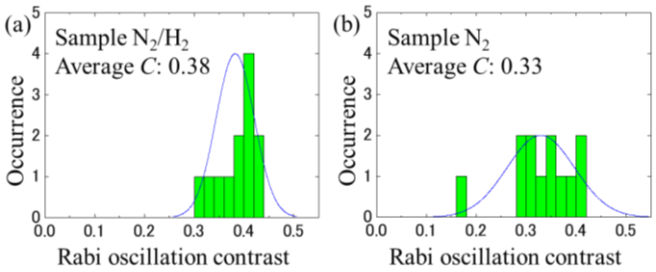

Fig 1. Histogram of Rabi oscillation contrast defined by (1) after nitrogen radical beam exposure using (a) mixture gas of N_2 (96%) + H_2 (4%) for Sample N_2/H_2 and (b) pure N_2 gas for Sample N_2.

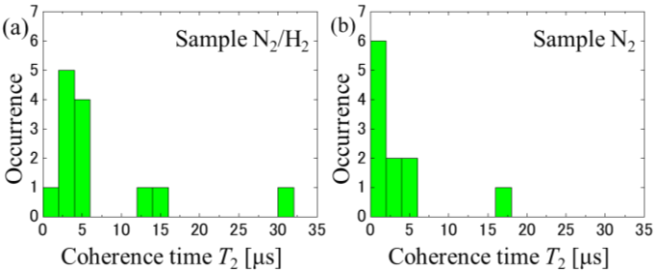

Fig 2. Histogram of estimated coherence time T_2 after nitrogen radical beam exposure on (a) Sample N_2/H_2 and (b) Sample N_2.

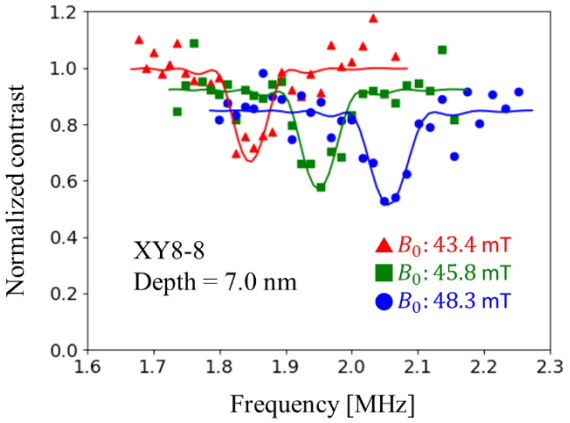

Fig 3. NMR spectra of ^{1}H nuclear spin detected by XY8-8 (64 π pulses) measurement using a single NV center under the N terminated surface of Sample N_2/H_2.

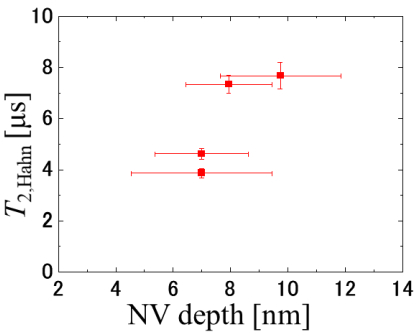

Fig 4. Plot of coherence time T_2 vs depth of NV centers extracted from the NMR spectra.